ISSN (Print) 1226-1750
ISSN (Online) 2233-6656
Journal of Magnetics 24(3), 437-447 (2019) https://doi.org/10.4283/JMAG.2019.24.3.437

Material Development of Perpendicular Recording for High Areal Density Hard Disk Drives

Kunpot Mopoung[1] and Sakuntam Sanorpim[1,2]*

[1]*Nanoscience and Technology, Graduate school, Chulalongkorn University, Phathumwan, Bangkok 10330, Thailand*
[2]*Department of Physics, Faculty of Science, Chulalongkorn University, Phathumwan, Bangkok 10330, Thailand*

(Received 13 June 2019, Received in final form 7 September 2019, Accepted 11 September 2019)

This review paper provides a survey of material development of perpendicular recording (or perpendicular magnetic recording, PMR) as it relates to the 'areal density' of hard disk drives (HDDs) with high amounts of information stored per unit area. Conventional longitudinal recording has reached its limits in terms of increasing the areal density. Hence, perpendicular recording promises to achieve high areal density, which is the current goal for both the academic and industrial sectors. Development of perpendicular recording can be considered in terms of the 3 primary parts of HDDs: the medium, write head and read head. Experimentation and computer simulations were used to optimize the parameters for improving the areal density of HDDs.

Keywords : Perpendicular recording, areal density, hard disk drives

1. Introduction

Magnetic material has long played an important role in data storage industry, especially in hard disk drives (HDDs). Since 1956, when the first commercial HDDs (IBM 350 RAMAC Disk Storage) were introduced by IBM [1], these HDDs have been the primary secondary storage device in computers and data centers, and also have been expected to continually grow in number of shipments in 2019 [2]. HDDs store information through the magnetization of a circular recording disk. Each domain or bit cell stores only one magnetization, which represents a binary number (0 or 1). On the recording disk, bit cells are usually aligned in two directions, with one positioned in a circumferential direction (down-track direction) and the other in a radial direction (cross-track direction). The density of the bit cells on the recording disk is celled the 'areal density'. The areal density has been developed over a long time [3-23], as shown in Fig. 1. Perpendicular recording (perpendicular magnetic recording, PMR) technology is one of the keys to increasing the areal density.

Perpendicular recording is a way to store magnetization in a direction perpendicular to the medium plate [24]. This approach allows the perpendicular recording to contain more data bit than a longitudinal recording. Although perpendicular technology has introduced many advantages compared with longitudinal recording technology since 1955, it was not successfully used in manufacturing for mass production until 2005 by Toshiba Co. [25].

In this review paper, we have focused on the development of perpendicular recording technology in the viewpoint of materials and their developments for the medium, write head and read head in the period of 1955 to present. Although, the perpendicular recording technology was intensively studied, especially for an academic perception, during the period from 2000 through 2010.

2. Brief History of Perpendicular Recording Technology

In 1955, the advanced disk file (ADF) project was started by San Jose Research Laboratory. The ADF project aimed to find the next generation of HDDs with ten time higher in data capacity and ten time faster in access time compared to the IBM 350 Disk Storage [26]. There were several technologies that were applied into the IBM 350 Disk Storage, such as a flying magnetic head that employed Bernoulli's principle to control the spacing between the head and the storage disk, called "head-to-media spacing". The flying head was key to reducing the head-

*Corresponding author: Tel: +66-2-2187541
Fax: +66-2-2531150, e-mail: sakuntam@gmail.com

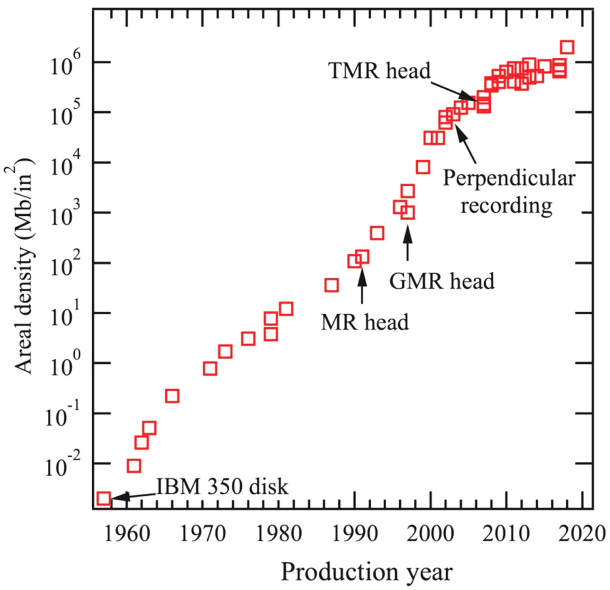

Fig. 1. (Color online) Development in the areal density of HDDs [3-23].

to-media spacing form 800 micro-inches (approximately 20 μm) to 250 (6.35 μm) micro-inches, providing the higher areal density [27]. With the flying head, the areal density went up to 520 bits per inch or 0.026 Mb/in^2 [28].

From the beginning, the ADF project considered using a perpendicular recording on a steel disk for IBM 1301 Disk Storage, but before its launch (in 1960), the ADF changed back to using aluminum disks based on the IBM 350 RAMAC longitudinal recording technology [26]. The reasons were that technology required a longer development time and that the magnetic properties of the steel disk were unpredictable.

In 1977, Iwasaki and Nakamura showed that it was possible to make a high areal density HDDs by using perpendicular recording technology [29]. They showed that a single pole-type head design was more suitable for the high areal density system. However, no one succeeded in increasing the areal density by using perpendicular technology at that time.

In addition, there were other technologies that got attention over the perpendicular recording technology to increase the areal density. For example, in 1979, IBM introduced IBM 3370, which consisted of the first thin-film read/write heads [30]. The thin-film heads used a lower current to write data and read faster than the old ferrite Metal-In-Gap (MIG) head. It was established that the size of the read/write head was reduced, and that the areal density was increased beyond 7.8 Mb/in^2 [28].

In 1990, the IBM 9345 disk storage was introduced with the first anisotropic magnetoresistive (AMR) read head, which used the magnetoresistive effect [31], discovered by Willian Thomson (Lord Kelvin) [32]. The MR effect results in changing electric resistance with an applied magnetic field. The AMR read head, which was made of NiFe ferromagnetic film, changed the MR ratio (electric resistance change, $\Delta R/R$) by approximately 2 % when the magnetic field was applied [33, 34]. Compared to a conversional head, the MR read head required less magnetic field to read and allowed the inductive write head to use fewer copper coils. As a result, the new head design led to an areal density of greater than 132 Mb/in^2 [35].

In 1997, a giant magnetoresistance (GMR) head was introduced by IBM [36]. The GMR involves the effect of two parallel ferromagnetic layers on the electric resistance, which was discovered in 1988 by Albert Fert and Peter Grünberg [37, 38]. When the magnetizations of the parallel ferromagnetic layers are aligned in an identical direction, the resistance will be decreased. However, the MR ratio will be increased to about 10 % [39] when there are unaligned magnetizations. The GMR head consisted of 4 layers, a free layer, a non-magnetic metal layer (spacer), a pinned layer and an anti-ferromagnetic layer. The GMR head increased the areal density to approximately 1000 Mb/in^2 or 1 Gb/in^2 in 1997 [35].

At that time, the goal of the industry had been to increase the areal density beyond 1.0 Tb/in^2 (1000 Gb/in^2). This goal had led to the perpendicular recording technology being considered to develop again.

3. Material Development for Perpendicular Recording Technology

The limit that the longitudinal approach meets when increasing the areal density is the tri-lemma limit. The tri-lemma limit is a trade-off between the signal-to-noise ratio (SNR) of the medium, the thermal stability and the writability [40]. Material development of perpendicular recording technology is based on the tri-lemma approach. This development can be considered in terms of 3 parts: (3.1) the read head, (3.2) write head and (3.3) medium.

3.1. Read head

Conventional GMR read heads have 4 multi-layers perpendicular to the disk, as shown in Fig. 2(a) and 2(b). The first layer is made of ferromagnetic material, which is called the free layer. The free layer exhibits variable magnetization, which is changed by the recording media's magnetic field. The second layer is a very thin, non-magnetic metal spacer usually made of metal, particularly copper. The thickness of this layer was less than the mean

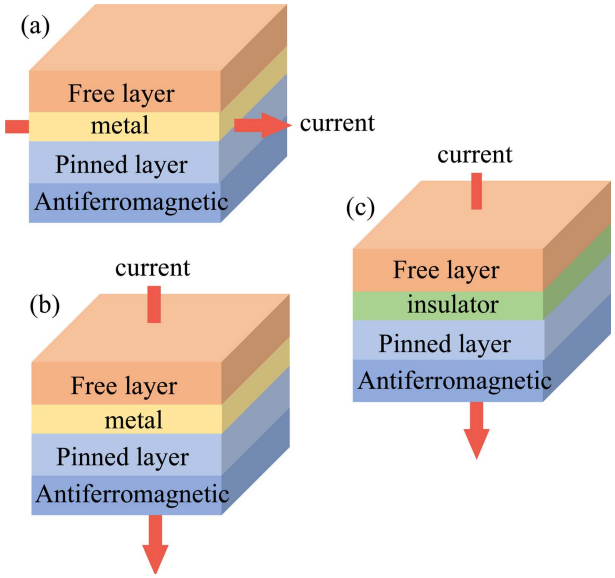

Fig. 2. (Color online) Schematic structures of (a) CIP-GMR, (b) CPP-GMR and (c) TMR geometries.

free path of an electron, which allows electric current to pass though it easily. The third layer is called the pinned or fixed layer. The fixed layer also made of ferromagnetic material, similar to the free layer, but its magnetization is fixed. To fix the magnetization of the pinned layer, a fourth layer is required. The fourth layer is made of an antiferromagnetic material, which exerts an antiferromagnetic exchange-coupled effect to maintain the direction of magnetization. It was well known that the ferromagnetic material for the free and pinned layer was usually NiFe [41-43].

Figure 2(a) shows schematic structure of a current-in-plane giant magnetoresistive (CIP-GMR) head sensor. Both ends of the CIP-GMR structure are contacted with magnetically hard electrodes, which are usually composed of alloy consisting of chromium, platinum, cobalt, and boron. To reduce the magnetic domain noise, the electrical current is applied in the longitudinal direction.

To increase the areal density (smaller grain of the bit cell), a new head structure was introduced. The current-perpendicular-to-plane (CPP) structure, as shown in Fig. 2(b), applies an electrical current in a perpendicular direction to the layer. This CPP-GMR structure has 2 primary advantages, which are, better temperature control and higher signal output. The CPP-GMR structure has more constant power consumption, which provides a stable temperature in the read head structure. The cross-sectional area of the CPP-GMR structure is also higher, which leads to higher sensitivity and higher signal output [45]. However, the CPP-GMR has a problem, that is, lower controllability of the hysteresis loop and magnetic domain [44].

The alternative CPP head design is a tunnel magnetoresistive (TMR) head, as shown in Fig. 2(c). The TMR head uses the tunnel magnetoresistance effect, which was discovered in 1975 by M. Julliere *et al.* [46]. The TMR effect occurs in a magnetic tunnel junction (MTJ). The MTJs have a thin insulator of a few nanometers between 2 ferromagnetic layers (pinned and free layers) instead of the metal layer in the GMR head structure. The TMR head allows only the electrons to tunnel though the potential barrier of thin insulator and into the subband of the same spin orientation. In the case of a parallel magnetic configuration, spin-up electrons, which make up the majority of the first layer, can tunnel easily into the second layer, which also has a majority of spin-up states. With an antiparallel configuration, fewer spin-up electrons can tunnel into the second layer, which has a minority of spin-up electron state. Thus, a parallel magnetic configuration exhibit resistance (R_P) lower than that of an antiparallel magnetic configuration (R_{AP}). A high MR ratio, which is identified by $(R_{AP}\text{-}R_P)/R_P$, represents a high sensitivity of the read head to a small magnetic field of medium.

The MTJ insulator layer is usually made up of AlO and MgO [47]. In case of AlO insulator layer, the tunnel electrons are scattered by the amorphous AlO structure, which has a disordered atomic arrangement. This causes the MR ratio of the AlO-based insulator MTJ to be less than 100 %. On the other hand, MgO is a single crystal, and electrons do not disperse, leading to a higher MR ratio. With a use of the MgO insulator layer, the MR ratio is increased up to approximately 140 % [48]. To fabricate the crystalline layer, the deposition of MgO barrier layers commonly requires ferromagnetic layers with a precise crystalline orientation. The ferromagnetic layers are usually made of Co, Fe or their alloys, with body-centered cubic (bcc) structure. To reduce the electron scattering at the interface, a (001)-oriented surface is suitable because of its relatively small lattice mismatch with MgO (001) [47, 49].

The structure of the MTJ in the TMR head is illustrated in Fig. 3. The antiferromagnetic (AF) layer is a seed layer made up of a few monolayers of Fe-Mn or Pt-Mn. The synthetic ferrimagnetic (SyF) structure consists of antiferromagnetically coupled Ferromagnetic/Non-magnetic/Ferromagnetic (FM/NM/FM) layers. Exchange biasing between the AF layer and the SyF structure makes the SyF structure into the pinned layer. This type of pinned layer is an important key to the TMR head because of its strong exchange bias. Unfortunately, a reliable AF/SyF

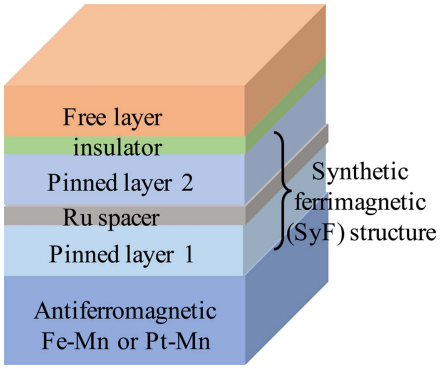

Fig. 3. (Color online) Schematic of the cross-sectional structure of an MTJ for practical applications. (layers are not to scale) [50].

has a face-centered cubic (fcc) (111) texture, while the MgO tunnel layer had a bcc structure. Because of differences in the crystal structures, depositing the MgO tunnel layer on the SyF pinned layer is difficult [50].

To obtain a single crystalline MgO tunnel layer, Djayaprawira *et al*. [50-53], developed a novel CoFeB/MgO/CoFeB MTJ by sputtering deposition method (Fig. 4) [51]. With this technique, the top and bottom CoFeB electrode layers were observed to exhibit an amorphous. The MgO tunnel layer was found to be (001)-preferred polycrystalline. This result is a very unusual because the MgO layer grown on other amorphous layers is normally amorphous. To investigate this growth mechanism, the *in situ* reflective high energy electron diffraction (RHEED) was used and the growth mechanism is displayed in Fig. 4 [54]. In Fig. 4(a), it was evident that at first, the MgO film was amorphous MgO. At a thickness of 1 nm, MgO begins to crystallize to the (001)-preferred texture, shown in Fig. 4(b). After the deposition of the CoFeB top layer (Fig. 4(c)), the 1.0-nm amorphous MgO exhibited the (001)-preferred crystal orientation, as shown in Fig. 4(d). Furthermore, the other advantage of the CoFeB amorphous is that it can be deposited on various underlayers, and on the standard SyF pinned layer.

These authors also reported a structural phase transformation in $Co_{60}Fe_{20}B_{20}$ from an amorphous to a bcc structure by an annealing process. Due to the influence from the MgO (001) layer, the $Co_{60}Fe_{20}B_{20}$ layer crystallized as bcc (001)-preferred polycrystalline after annealing at 250 °C, even if the thermodynamically stable crystal structure of $Co_{60}Fe_{20}B_{20}$ had an fcc structure. Not only does the MgO (001) have an influence on the CoFeB structure, but a cap layer, which is the layer deposited on the top CoFeB electrode, also influences the crystallization of CoFeB. Tsunekawa *et al*. demonstrated the deposition of various materials, such as NiFe, Ru and Ta, for the cap layer [52]. They reported that a Ru or Ta cap layer, which is the same material as the space layer in the SyF structure, does not show an influence on the CoFeB electrode (Fig. 5(a)). Additionally, a $Ni_{80}Fe_{20}$ (permalloy) cap layer, which has a fcc structure, was significantly affected upon the crystallization of CoFeB after annealing at 200 °C. Thus, when the annealing temperature increases up to 250 °C, CoFeB, which has a stable fcc structure, does not change to bcc structure (Fig. 5(b)). This behavior causes the MTJ with a Ru or Ta cap layer to exhibit a giant MR ratio.

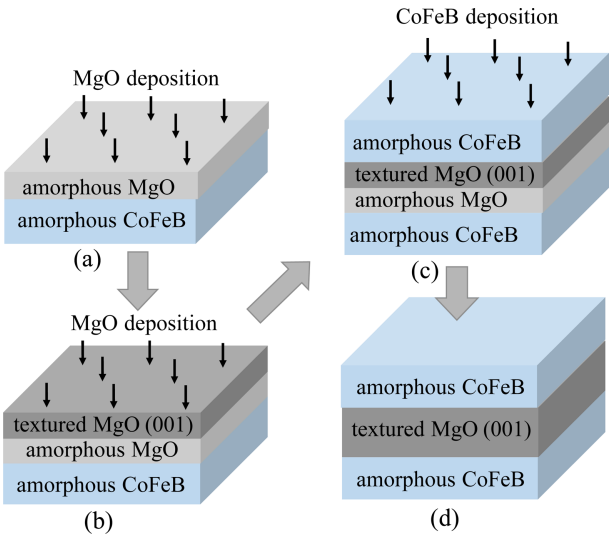

Fig. 4. (Color online) The growth process for a CoFeB/MgO/CoFeB MTJ film. (layers are not to scale) [50, 54].

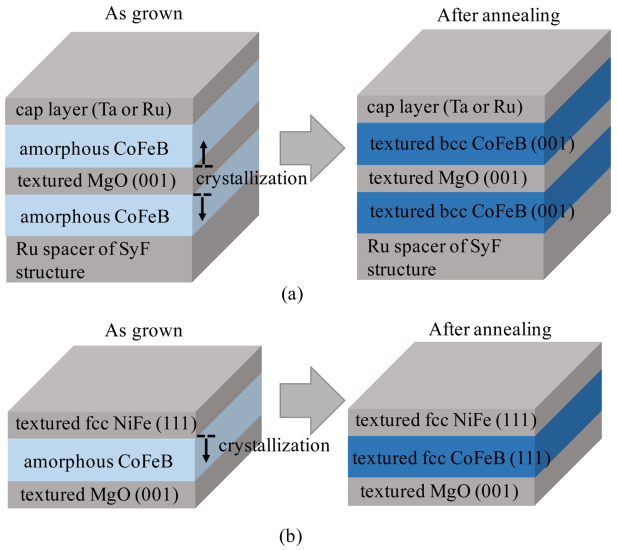

Fig. 5. (Color online) The structure of CoFeB/MgO/CoFeB MTJ in the as-grown state and after annealing at 250 °C. (a) The cap layer is made of Ta or Ru. (b) The cap layer is $Ni_{0.8}Fe_{0.2}$ (permalloy). (layers are not to scale) [50, 54].

The MR ratio of this MTJ also depends on the composition and the thicknesses of the CoFeB film. For example, Lee Y. M. reported that the MR ratio of MTJ, which consists of 4- and 4.3-nm-thick $(Co_{25}Fe_{75})_{80}B_{20}$ electrodes and a 2.1-nm-thick MgO tunnel layer and was annealed at 475 °C, is 500 % at room temperature (300 K) and would reach up to 1010 % at 5 K [55]. Consequently, with the material development of the TMR head, the areal density of HDD was raised to 200-520 Gb/in^2 for the MgO-based tunnel layer [53, 56].

3.2. Write head

In perpendicular recording technology, the magnetizations of the recording layer are perpendicular to the recording disk. The writing recording field must align in the identical direction (perpendicular to the recording disk) to change the magnetization of the recording layer. Iwasaki and Nakamura suggested the write head structure for the perpendicular recording medium, which was called a 'pole-type write head' [29, 57]. To complete the loop of magnetic flux, the pole-type head has a main pole and a return pole. The writing magnetic field of the pole-type head is generated when the electrical current is applied to copper coils. The writing magnetic field goes out from the main pole and comes back to the return pole. However, this design aligned the main pole and return pole on opposite sides of the recording disk. The main pole has a small width to create a high magnetic flux density. Additionally, the return pole is much wider compared with the main pole to avoid causing a disturbance on another bit cell. This design showed the possibility to archive the areal density of 20 kilobits (kb) per inch [58]. However, the pole-type head, which had the main pole and return pole on opposite side of the recording medium disk, was difficult to fabricate in real devices.

In 1982, Ohtsubo and Satoh introduced a new pole-type head with single sided structure, which called a 'trapezoidal head' or a 'tapered pole head' [59]. Instead of using the opposite side of poles, a soft magnetic underlayer (SUL) was added to underneath the recording layer to complete the loop of magnetic flux. The cooperation with the SUL moves the return pole to the same side of the main pole and allows for the use of both sides of the disk for the recording layer. The purpose of the SUL is to create an image head, and the magnetic writing field occurs in the gap between the real and image heads (Fig. 6). This concept leads the maximum writing magnetic field to be equal to $4\pi M_S$, while the maximum writing field from the ring-type head in longitudinal recording head is equal to $2\pi M_S$, where M_S is the saturation magnetization of the write head material [60].

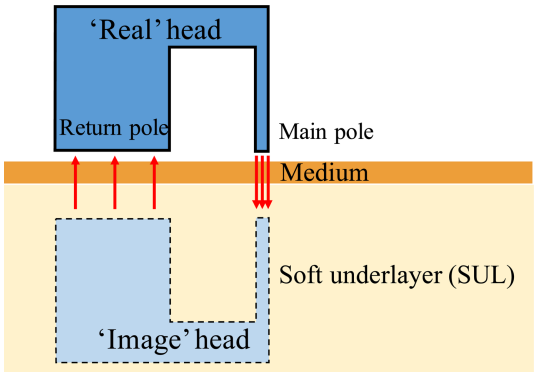

Fig. 6. (Color online) Schematic of the magnetic imaging head in the SUL.

To obtain the maximum field from the tapered pole-type head, the write head was developed in terms of the following 2 important parameters: (3.2.1) the magnitude of the write magnetic field in the recording layer and (3.2.2) the gradient of the write magnetic field.

3.2.1. Magnitude of the write magnetic field

To reach a high magnitude of the magnetic write field, the write head should be made of high-saturation magnetization material. The saturation magnetization (M_S) is the maximum of a generated magnetic field of a material when an external magnetic field is applied. Therefore, with the same electric current applied to copper coils, the high-saturation magnetization write head can produce a higher writing magnetic field than the head made of low-saturation magnetization material. The current high-saturation magnetization material is a Co-Fe alloy, which can reach up to about 2.45 T/μ_0 [61]. Additionally, there are several reports that show the alternative materials which are promising to produce a higher saturation magnetization for the write head, such as the FeCoAlO [62], α'-$Fe_8(NC)$ [63] and $Fe_{16}N_2$ [64].

Furthermore, the design of the write head is also important for obtaining a high magnitude of the write magnetic field. In early 2000's, the concept of a multi-tapered pole head was purposed. The multi-tapered pole head is the head which has a tapered shape in both the down-track and cross-track directions. The different shapes of the multi-tapered pole head are shown in Fig. 7 [40]. Head (a) has a stepped structure, which is actually not a multi-tapered pole head, but the magnetic write field is very similar to the multi-tapered pole [65]. However, it is also considered as a multi-tapered pole. Head (b) has two sides with tapered shape, with the same breakpoint length or neck [66]. Where, breakpoint length is defined as the distance between the write pole and the tapered nick. Head (c) has two sides with tapered shapes, but it has no

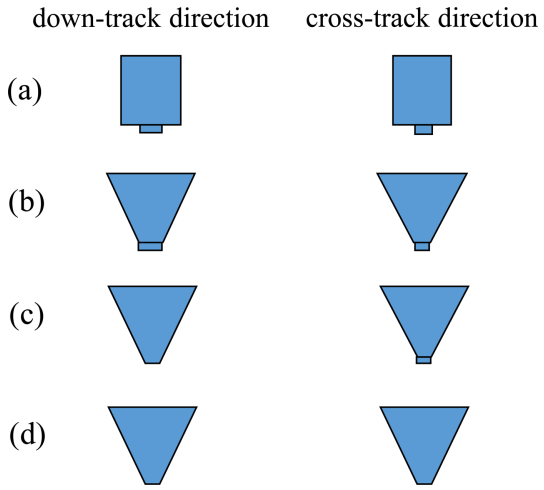

Fig. 7. (Color online) Schematic of several types of multi-tapered pole heads [40].

neck (no breakpoint) in the down-track direction [67]. Head (d) has two sides with the tapered shape without the breakpoint length or neck [68]. The write field from head (a) is the lowest, whereas this design is the easiness to fabricate. So, the design of head (b), (c) and (d) are chosen for the high areal density perpendicular recording write head. The different in these head designs are the different in the breakpoint length.

Many publications have shown an optimization of the multi-tapered pole design. The first optimization is the size of the main pole. Gao and Bertram showed the reduction of the write magnetic field with a smaller write head, especially when it was smaller than 120 nm [69]. To overcome this limit, the length of the breakpoint must be reduced. These researchers compared the write magnetic fields for different lengths of the breakpoint and different pole widths. The 120-nm width write head with the breakpoint length of 200 nm has a more highly normalized write magnetic field than the 320-nm width one with the same breakpoint length. The write magnetic field with a 120-nm width and 40-nm breakpoint length head was clearly higher. However, the reduction in the breakpoint length led to a broadening of the magnetic write field in the recording layer due to the greater number of surface charges on the side of the tapered nick.

3.2.2. The Gradient of the write magnetic field

The gradient of the magnetic field is defined as the change rate of the magnetic field per distance. A write head with a high gradient of magnetic field is good for a small gain size in a high areal density medium. The high gradient of the magnetic field prevents the data erasure problem in adjacent bits. To increase the gradient of the write magnetic field, careful design of shields and coils is needed. Several coil designs have been developed [40]. The unbalanced coil design induces an unbalanced write magnetic field. This unbalanced magnetic field causes the erasure of stored data in the medium. To counter this problem, the balanced pancake design and the helical coils were used.

A shield is also important for increasing the gradient of the magnetic field. The conventional model of a shield is a trailing shield. The write magnetic field from the tapered pole head can be varied by the gap between the shield and the pole head. Greaves *et al*. showed that the distribution of the write field becomes narrower when the trailing shield is closer to the pole head [70]. The highest magnetic field comes from the head with a 30-nm trailing gap. Notably, this shield reduces the vertical magnetic field from the pole-type head by 2 kOe comparing with no trailing shield.

In 2012, Bashir *et al.* used a computer simulation to optimize the head design for a high areal density medium. They reported that the head with their optimizations can produce an effective write magnetic field for media with 2.5 Tb/in^2 of areal density [71].

3.3. Medium

A medium of an HDD is made of an anisotropic magnetic material. An anisotropic material has a preferential direction for its magnetization (easy axis), while an isotropic one has no easy axis. In longitudinal recording medium, the easy axis aligns with the plane of the recording disk, whereas in perpendicular recording, the easy axis aligns perpendicular to the disk. The conventional longitudinal recording medium used a CoCr alloy which has a granular structure that consists of several magnetic grains or clusters. The magnetic grains are randomly shaped over a rage from 15 to 40 nm [72-73]. These imperfections cause noise in the reading signal. The signal-to-noise ratio (*SNR*) of the media is approximately equal to 10 $log(N)$, where N is the number of grains in a bit [74]. The *SNR* is one of the important parameters representing the performance of the recording media. To increase the *SNR* of the recording media, the number of gains per bit area must be increased, which means the gain size and the gain magnetization distribution must be reduced.

The other key parameter is the magnetic anisotropy energy, which is defined as the amount of energy needed to change the direction of a bit's magnetization. This energy is equal to K_uV, where K_u is the anisotropy constant and V is the volume of the grain. When the anisotropy energy K_uV is low, the thermal energy (k_BT) begins to have an effect. This influence leads to the reversion of the

grain's magnetization without applying any external magnetic field, which is called 'superparamagnetism'. In late 1990's, the superparamagnetic limit for longitudinal recording medium is predicted over a range from 40 to 60 Gb/in^2 [75-76]. To solve this problem, perpendicular recording was considered.

According to Iwasaki and Nakamura, the ring-type head is not suitable for perpendicular recording [57]. A suitable tool should be a single pole-type head which produces a magnetic field straight to the medium and returning to the head again. Thus, the medium for perpendicular recording has to add a soft magnetic underlayer (SUL) under a recording layer to maintain the part of the magnetic flux and increase the write field. The SUL is made of high-permeability material.

In cooperation with the SUL, the pole-type head can produce twice the maximum magnetic field compared with longitudinal recording. This increase in the field magnitude can be understood by assuming infinite permeability for the SUL. In this case, the currents in the write head, which generate the vertical magnetic field, create a mirror 'image' in the SUL, which can be modeled by a second imaginary write head, as shown in Fig. 6. The higher upper limit for the pole-type head's magnetic field allows for a higher K_u material for the recording medium. In effect, the perpendicular recording medium can reduce the grain size with less of a superparamagnetic effect.

In 1990's, the CoCr [78] and its alloys (e.g., CoCrNb [79], CoCrPt, CoCrTa [80-81]) were studied for use in perpendicular media. To obtain grain boundaries, the Cr composition was increased. A high Cr composition caused a reduction in the anisotropy constant, K_u, and the grain size could not be decreased less than 12 nm, while the longitudinal recording medium had a grain size of approximately 8-9 nm [74]. Thus, perpendicular recording technology was not considered to be a product with mass commercial potential until the longitudinal recording medium reached the areal density limit of 130 Gb/in^2 in early 2000's [77].

The practical design of the perpendicular medium is approximately displayed in Fig. 8. The substrate of the medium platter was made of an AlMg alloy or glass with an amorphous NiP electrode layer. To attach smoothly to the SUL layer and the upper layers, the next layer is an adhesion layer or interface layer, which is usually made of Ta, Ti or their alloy. The intermediate layer is used to reduce the exchange-coupled effect between the SUL layer and the recording layer. Another purpose of this layer is to provide an epitaxial growth condition for a recording layer. The recording layer for the perpendicular medium made of the hexagonal Co-based alloy has the

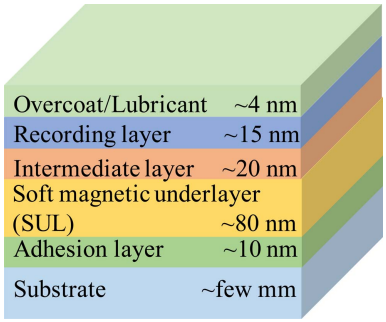

Fig. 8. (Color online) Schematic of layers of the perpendicular recording medium. (layers are not to scale) [74].

(0002) orientation. For this reason, the intermediate layer should have the fcc (111) [82] or hcp (0002) orientation texture [83]. The top layer of the perpendicular recording medium is coated with a diamond-like carbon (DLC) layer and a lubricant layer with a thickness of a few nanometers. The purpose of these layers is to reduce media wear caused by the flying head. All the layers are deposited by a sputtering process except for the lubricant layer, which is deposited using a dip-coat process.

The material development of the perpendicular recording medium can be considered in terms of three parts.

3.3.1. Soft magnetic underlayer (SUL)

Due to the SUL material is made of a larger magnetization material and it is thicker than the recording layer, it raises the noise in the playback signal, which comes from the SUL domain walls. The noise problem was one of the serious problems for the perpendicular recording medium because the domain that causes the noise spike can move, and thus, it cannot be marked as a bad sector on the HDD [84]. To counter this problem, the first solution is a magnetic biasing, which was introduced by Dmitri Litvinov *et al*. [85]. Magnetic biasing forces the SUL into a single magnetic domain. This process can employ either an external magnetic field or built-in permanent magnets in the SUL. The magnetic biasing helps the SUL reach complete saturation. For example, two permanent NdFeB magnets are placed in the vicinity of the medium, which must be far enough away to avoid the effect on the recording head (approximately 2 cm). This technique could reduce the noise of the SUL by at least 10 dB.

The second solution for the SUL noise problem is finding a novel material that has fewer domains. Honda *et al.* noted that the medium with a Co-Ta-Zr SUL shows low noise [86]. Co-Ta-Zr, with Ta concentration of approximately 6 to 12 % and Zr concentration of approximately 2 to 6 %, is one of the candidate materials for SULs [74].

The alternative solution to eliminate SUL noise is to employ a laminated SUL structure (SUL multi-layer). The laminated SUL was found to have a magnetostatic interaction between adjacent magnetic layers, which leads to low coercivity. Hence, this structure has a much lower spike noise than a single-layer SUL [74]. For example, Acharya *et al.* investigated the spike noise on a sample with CoTaZr SULs and with an anti-parallel-coupled (APC) SUL [87]. The results showed that the sample containing the APC SUL has a lower spike noise compared to a single SUL.

The SULs produce not only the domain-boundary noise but also cause an exchange interaction with the recording layer, which can lead to large noise during a read process. An intermediate layer is needed to eliminate this exchange interaction. So the intermediate layer was introduced to reduce the noise.

3.3.2. Intermediate layer

In 2000, there are several publications reported that only a few nanometer-thick intermediate layer can reduce the magnetic interaction between the SUL and the recording layers [88-90]. For example, Honda *et al.* showed that introducing a 2-nm-thick nonmagnetic intermediate layer can reduce the magnetic interaction between a CoTaZr SUL and a CoCrPt recording layer, which reduces the noise by approximately 20 % [91].

The intermediate layer is also used to induce a structure in the perpendicular recording layer, which is usually made of the hcp Co-based alloy [92]. The Co-alloy-based recording layer has an easy c-axis in the hcp ([0002]-orientation). The c-axis oriented dispersion of the recording layer ($\Delta\theta_{50}$), which was observed by using X-ray diffraction rocking curves, represents the quality of the magnetic recording layer. A narrow dispersion (or small $\Delta\theta_{50}$) leads to a high coercivity, H_c and a high SNR in the medium [93].

To reduce $\Delta\theta_{50}$, the intermediate layer must be optimized. The first optimization is performed on the thickness of intermediate layer. Some papers report on variations in the thickness of the Ru intermediate layer with a CoPtCrO recording layer [93-94]. They noted that an increase in the Ru thickness leads to a smaller $\Delta\theta_{50}$. However, a thicker intermediate layer causes increasing head-to-keeper spacing, which leads to a reduction in the write field. Thus, an optimized thickness is needed. Choe *et al.* reported that Ta/Ru intermediate layers for the Co recording layer can obtain a $\Delta\theta_{50}$ of 3° [93].

3.3.3. Recording magnetic layer

Since the 1970s, CoCr-alloys, such as CoCrNb [58], CoCrPt and CoCrTa [80-81], have been used in perpendicular recording layer. One major barrier to using the CoCr alloy is the switching field (the field required to change the magnetization) [74]. The low switching field of the CoCr alloy material make it easy to change the magnetization of the recording layer. Some of the gains in the recording bit could be reversed, leading to high noise in the medium. The improvement of the CoCr alloy with high K_u and high thermal stability is an importance key to countering this problem. Some studies have shown that a decrease in Cr concentration increases K_u [95]. However, reducing the Cr concentration leads to problem in the exchange-coupled interaction [96].

CoCrPt-oxide-based materials were introduced as candidates for use in the recording magnetic layer. Additional oxide materials, such as Si oxide and Cr oxide, surround the CoCr alloy grain as a grain boundary. The oxide-based grain boundary effectively isolates the CoCr alloy recoding gains. This boundary reduces the exchange-coupled interaction between the recording grains without reducing the Cr concentration. The addition of oxide-based material can reduce the recording gain size and increase the SNR simultaneously [97-99].

Even though, a high K_u medium is needed to increase the *SNR*, it causes a problem in the writability. To improve the writability of the recording layer without decreasing the K_u or thermal stability, an exchange-coupled composite (ECC) medium was introduced [100-101]. The ECC medium consists of a low K_u layer, called a soft layer, and a high K_u layer, called a hard layer. The soft layer, which is deposited on the top, has an exchange interaction with the hard layer. When magnetic writing field is applied, the soft layer will be switched at first. After that, the soft layer will induce the hard layer switching via the exchange interaction. This mechanism requires a lower writing magnetic field than a single layer magnetic recording layer. The ECC medium not only reduces the switching field to improve the writability but also can improve the thermal stability [102].

In 2008, Qiu *et al*. developed an ECC medium by using multi-layer nanocomposite structures [103]. They used Ta/Ru/$CoCr_1$/FeCoTaCr as soft magnetic layers and Ta/Ru/CCo_1/CoCrPt-SiO_2/$CoCr_2$/FeCoTaCr/C for the hard layer and performed a comparison with a conventional perpendicular medium. The noise of the ECC remains constant when the linear density of the recording layer is increased, which leads to the ECC having a higher SNR. Furthermore, Greaves *et al*. used a computer simulation to determine and optimize suitable parameters for the ECC medium [104]. They reported that an increase in the oxide content of the ECC medium can improve the SNR.

Table 1. Comparison of specifications for a hard disk drive (HDD) and a solid-state drive (SDD) [109].

Attribute	HDD	SSD
Power Draw	6-7 watts	2-3 watts
Maximum Capacity	2 TB for notebooks and 10 TB for desktops	1 TB for notebook and 4 TB for desktops
Write Speed	50-120 MB/s	200-550 MB/s
Failure Rate	1.5 million hrs	2.0 million hrs
Cost	$0.03 per GB	$0.20 per GB

With an oxide concentration of 32.8 %, the minimum bit area of the recording bit is 60 nm × 12.1 nm = 726 nm^2, or 890 Gb/in^2 in areal density.

4. Future View

Although perpendicular recording technology is expected to overcome the tri-lemma limit to increase the areal density, no publications about high areal density HDDs of over 1 Tb/in^2 exist. The big problem is reducing the bit size without reducing the SNR and thermal stability. Other design media are being introduced to solve this problem, such as heat-assisted magnetic recording (HAMR) [105], track discrete medium (TDM) [106], shingled magnetic recording (SMR) [107] and bit patterned media (BPM) [108].

Another storage device has begun to replace the HDD in computers, such as a solid-state drive (SSD). Comparation of specifications for SSD and HDD is shown in Table 1 [109]. Main advantage of HDD over SSD is a lower cost per areal density. To keep this advantage, an increasing of the areal density is needed to be simultaneously improved.

5. Conclusions

Material development of perpendicular recording medium is reviewed in this paper. To maintain its advantage over other recording technologies, such as solid-state drives (SSDs) or memory cards, the areal density must be increased continually. The areal density has a tri-lemma limit consisting of the SNR, thermal stability and writability. To overcome this problem, three primary parts (the read head, write head and medium) of HDDs must be subject to research in relation to their materials and design.

With the cooperation of the TMR read head, pole-type write head, anti-parallel-coupled soft underlayers and ECC recording layer, the areal density can be increased and exceed the areal density obtained with conventional longitudinal recording technology. As an expectation, industry has already been shipping drive over 1.0 Tb/in^2 to the market at the moment [110]. To increase the areal density, another technology is required. Although the performance of SSDs is better than that of HDDs (in terms of energy efficiency and write speed), the capacity (areal density) per cost of the HDD still has an advantage over the SDD.

Acknowledgments

This work was supported by the Development and Promotion of Science and Technology Talents Project (DPST); and the 90th Anniversary of Chulalongkorn University Fund (the Ratchadaphiseksomphot Endowment Fund). The authors would like to convey their thank to the Ph.D. Program in Nanoscience and Technology, Graduate School, Chulalongkorn University, Phongbandhu Sritonwong and to staffs of the Advanced Material Physics Research Group (AMPRG), department of Physics, faculty of Science, Chulalongkorn University for their useful suggestions.

References

[1] https://www.ibm.com/ibm/history/exhibits/storage/storage_350.html/.
[2] https://www.kasikornbank.com/international-business/en/Thailand/IndustryBusiness/Pages/201902_Thailand-_HDD_outlook2019.aspx/.
[3] http://www.digitalpreservation.gov/meetings/documents/storage14/Fontana_Volumetric%20Density%20Trends%20for%20Storage%20Components%20--%20LOC%2009222014.pdf/.
[4] https://www-03.ibm.com/ibm/history/exhibits/storage/storage_magnetic.html/.
[5] https://www-03.ibm.com/ibm/history/exhibits/storage/storage_basic.html
[6] http://www.computerhistory.org/storageengine/thin-film-heads-introduced-for-large-disks/.
[7] http://www.computerhistory.org/storageengine/magneto-resistive-read-head-hdd-introduced/.
[8] https://manualzz.com/doc/8231872/cinemastar-c5k250-data-sheet/.
[9] https://www.storagereview.com/hgst_ultrastar_7k6000_hdds_now_shipping/.
[10] https://documents.westerndigital.com/content/dam/doc-library/en_us/assets/public/western-digital/product/data-center-drives/ultrastar-sas-series/data-sheet-ultrastar-he8.pdf/.
[11] https://documents.westerndigital.com/content/dam/doc-library/en_us/assets/public/western-digital/product/data-center-drives/ultrastar-dc-hc500-series/data-sheet-ultrastar-dc-hc520.pdf/.

[12] https://documents.westerndigital.com/content/dam/doc-library/en_us/assets/public/western-digital/product/data-center-drives/ultrastar-sas-series/data-sheet-ultrastar-archive-ha10.pdf?_ga=2.55325867.1413518244.1567093639-255162793.1566973941/.
[13] https://documents.westerndigital.com/content/dam/doc-library/en_us/assets/public/western-digital/product/data-center-drives/ultrastar-sas-series/product-manual-ultrastar-c15k600.pdf/.
[14] https://documents.westerndigital.com/content/dam/doc-library/en_us/assets/public/western-digital/product/data-center-drives/ultrastar-sas-series/data-sheet-ultrastar-c10k900.pdf?_ga=2.244182341.190040264.1546296136-1117608820.1543241049/.
[15] https://www.datori.lv/docs/eB7M/.
[16] https://docs-emea.rs-online.com/webdocs/00bb/0900766b800bb67c.pdf/.
[17] http://www.toshiba.co.jp/about/press/2008_09/pr1001.htm/.
[18] http://www.cdrlabs.com/news/western-digital-launches-industrys-first-2tb-hard-drives.html/.
[19] http://www.cdrlabs.com/reviews/hitachi-deskstar-5k3000-2tb-hard-drive.html/.
[20] https://blog.seagate.com/uncategorized/hamr-next-leap-forward-now/.
[21] http://www.hitachi.com/New/cnews/071015a.pdf/.
[22] http://ieeexplore.ieee.org/stamp/stamp.jsp?tp=&arnumber=662412/.
[23] https://www.extremetech.com/computing/58672-future-storage-the-view-from-2001/6?print/.
[24] S. Iwasaki, IEEE Trans. Magn.**16**, 71 (1980).
[25] https://www.toshiba.co.jp/about/press/2004_12/pr1401.htm/.
[26] A. S. Hoagland, IEEE Trans. Magn. **39**, 1871 (2003).
[27] https://www.ibm.com/ibm/history/exhibits/storage/storage_1301.html/.
[28] https://www.ibm.com/ibm/history/exhibits/storage/storage_magnetic.html/.
[29] S. Iwasaki and Y. Nakamura, IEEE Trans. Magn. **13**, 1272 (1977).
[30] https://www.ibm.com/ ibm/history/exhibits/storage/storage_3370.html.
[31] https://whatit.info/en/wiki/IBM_2311/.
[32] T. William, Proc. R. Soc. Lond. **8**, 546 (1857).
[33] E. V. Buzaneva and P. Scharff, Frontiers of Multifunctional Nanosystems, NATO Science Series II: Mathematics, Physics and Chemistry, Springer Netherlands (2002) pp 433-434.
[34] L. Jogschies, D. Klaas, R. Kruppe, J. Rittinger, P. Taptimthong, A. Wienecke, L. Rissing, and M. C. Wurz, Sensors **15**, 28665 (2015).
[35] https://www.computerhistory.org/storageengine/magnetoresistive-read-head-hdd-introduced/.
[36] https//www.ibm.com/ibm/history/history/year_1997.html/.
[37] M. N. Baibich, J. M. Broto, A. Fert, F. Nguyen Van Dau, F. Petroff, P. Etienne, G. Creuzet, A. Friederich, and J. Chazelas, Phys. Rev. Lett. **61**, 2472 (1988).
[38] G. Binasch, P. Grünberg, F. Saurenbach, and W. Zinn, Phys. Rev. B **39**, 4828 (1989).
[39] H. Fukuzawa, H. Iwasaki, K. Koi, and M. Sahashi, J. Magn. Magn. Mater. **298**, 65 (2006).
[40] Y. Kanai and K. Yamakawa, J. Magn. Magn. Mater. **321**, 518 (2009).
[41] G. Choe and S. Gupta, Appl. Phys. Lett. **70**, 1766 (1997).
[42] H. Kanai, K. Yamada, K. Aoshima, Y. Ohtsuka, J. Kane, M. Kanamine, J. Toda and Y. Mizoshita, IEEE Trans. Magn. **32**, 3368 (1996).
[43] N. Smith, A. M. Zeltser, D. L. Yang, and P. V. Koeppe, IEEE Trans. Magn. **33**, 3385 (1997).
[44] K. Nagasaka, Y. Seyama, R. Kondo, H. Oshima, Y. Shimizu, and A. Tanaka, Fujitsu Sci. Tech. J. **37**, 192 (2001).
[45] J. Bass and W. P. Pratt, J. Magn. Magn. Mater. **200**, 274 (1999).
[46] M. Julliere, Phys. Lett. A **54**, 225 (1975).
[47] J.-G. (Jimmy) Zhu and C. Park, Mater. Today **9**, 36 (2006).
[48] J. Kanak, T. Stobiecki, A. Thomas, J. Schmalhorst, and G. Reiss, Vacuum **82**, 1057 (2008).
[49] S. Yuasa, A. Fukushima, H. Kubota, Y. Suzuki, and K. Ando, Appl. Phys. Lett. **89**, 042505 (2006).
[50] S. Yuasa and D. D. Djayaprawira, J. Phys. Appl. Phys. **40**, R337 (2007).
[51] D. D. Djayaprawira, K. Tsunekawa, M. Nagai, H. Maehara, S. Yamagata and N. Watanabe, Appl. Phys. Lett. **86**, 092502 (2005).
[52] K. Tsumekawa, D. D. Djayaprawira, M. Nagai, H. Maehara, S. Yamagata, and N. Watanabe, INTERMAG Asia 2005. Digests of the IEEE International Magnetics Conference, Nagoya, Japan (2005).
[53] Y. S. Choi, Y. Nagamine, K. Tsunekawa, H. Maehara, and D. D. Djayaprawira, Appl. Phys. Lett. **90**, 012505 (2007).
[54] S. Yuasa, Y. Suzuki, T. Katayama, and K. Ando, Appl. Phys. Lett. **87**, 242503 (2005).
[55] Y. M. Lee, J. Hayakawa, S. Ikeda, F. Matsukura, and H. Ohno, Appl. Phys. Lett. **90**, 212507 (2007).
[56] https://gizmodo.com/western-digital-announces-record-breaking-hard-drive-de-312156/.
[57] S. Iwasaki and Y. Nakamura, IEEE Trans. Magn. **14**, 436 (1978).
[58] S. Iwasaki, Y. Nakamura, and H. Muraoka, IEEE Trans. Magn. **17**, 2535 (1981).
[59] A. Ohtsubo and Y. Satoh, IEEE Trans. Magn. **18**, 1173 (1982).
[60] S. Khizroev and D. Litvinov, J. Appl. Phys. **95**, 4521 (2004).
[61] H. Shokrollahi and K. Janghorban, J. Mater. Process. Technol. **189**, 1 (2007).
[62] I. Tagawa, S. Ikeda, and Y. Uehara, Fujitsu Sci. Tech. J. **37**, 164 (2001).
[63] M. Mehedi, Y. Jiang, P. K. Suri, D. J. Flannigan, and J.-P. Wang, J. Phys. D: Appl. Phys. **50**, 37LT01 (2017).

[64] J. P. Wang, N. Ji, X. Liu, Y. Xu, C. Sanchez-Hanke, Y. Wu, F.M.F. de Groot, L.F. Allard, E. Lara-Curzio, IEEE Trans. Magn. **48**, 1710 (2012).
[65] S. Takahashi, K. Yamakawa, and K. Ouchi, Tech Rep IEICE **25.36**, 1 (2001).
[66] K. Z. Gao and H. N. Bertram, IEEE Trans. Magn. **38**, 3521 (2002).
[67] Y. Kanai, R. Matsubara, H. Watanabe, H. Muraoka, and Y. Nakamura, IEEE Trans. Magn. **39**, 1955 (2003).
[68] K. Ise, S. Takahashi, K. Yamakawa, and N. Honda, IEEE Trans. Magn. **42**, 2422 (2006).
[69] K. Gao and H. N. Bertram, J. Appl. Phys. **91**, 8369 (2002).
[70] S. Greaves, Y. Kanai, and H. Muraoka, IEEE Trans. Magn. **42**, 2408 (2006).
[71] M. A. Bashir, T. Schrefl, J. Dean, A. Goncharov, G. Hrkac, D. A. Allwood, and D. Suess, J. Magn. Magn. Mater. **324**, 269 (2012).
[72] M. Yu, M. F. Doerner, and D. J. Sellmyer, IEEE Trans. Magn. **34**, 1534 (1998).
[73] J. E. Wittig, T. P. Nolan, C. A. Ross, M. E. Schabes, K. Tang, R. Sinclair, and J. Bentley, IEEE Trans. Magn. **34**, 1564 (1998).
[74] S. N. Piramanayagam, J. Appl. Phys. **102**, 011301 (2007).
[75] S. H. Charap, P. L. Lu, and Y. He, IEEE Trans. Magn. **33**, 978 (1997).
[76] K. Stoev, F. Liu, X. Shi, H. C. Tong, Y. Chen, C. Chien, Z. W. Dong, M. Gibbons, S. Funada, P. Prabhu, H. Nguyen, D. Wachenschwnz, L. Mei, M. Schultz, S. Malhotra, B. Lal, J. Kimmal, M. Russak, A. Talalai, and A. Varlahanov, IEEE Trans. Magn. **37**, 1264 (2001).
[77] G. Choe, J. N. Zhou, B. Demczyk, M. Yu, M. Zheng, R. Weng, A. Chekanov, K. E. Johnson, F. Liu, and K. Stoev, IEEE Trans. Magn. **39**, 633 (2003).
[78] N. Honda, J. Ariake, K. Ouchi, and S. Iwasaki, IEEE Trans. Magn. **30**, 4023 (1994).
[79] N. Honda, J. Ariake, K. Ouchi, and S. Iwasaki, IEEE Trans. Magn. **34**, 1651 (1998).
[80] Y. Hirayama, M. Futamoto, K. Kimoto, and K. Usami, IEEE Trans. Magn. **32**, 3807 (1996).
[81] Y. Hirayama, Y. Honda, T. Takeuchi, and M. Futamoto, IEEE Trans. Magn. **35**, 2766 (1999).
[82] S. N. Piramanayagam, H. B. Zhao, J. Z. Shi, and C. S. Mah, Appl. Phys. Lett. **88**, 092506 (2006).
[83] S. N. Piramanayagam, H. B. Zhao, J. Z. Shi, and C. S. Mah, Appl. Phys. Lett. **88**, 092501 (2006).
[84] A. Kikukawa, K. Tanahashi, Y. Honda, Y. Hirayama, and M. Futamoto, J. Magn. Magn. Mater. **235**, 68 (2001).
[85] D. Litvinov, M. H. Kryder, and S. Khizroev, J. Magn. Magn. Mater. **232**, 84 (2001).
[86] Y. Honda, A. Kikukawa, Y. Hirayama, and M. Futamoto, IEEE Trans. Magn. **36**, 2399 (2000).
[87] B. R. Acharya, J. N. Zhou, M. Zheng, G. Choe, E. N. Abarra, and K. E. Johnson, IEEE Trans. Magn. **40**, 2383 (2004).
[88] W. Peng, R. H. Victora, J. H. Judy, K. Gao, and J. M. Sivertsen, J. Appl. Phys. **87**, 6358 (2000).
[89] A. G. Roy, D. E. Laughlin, T. J. Klemmer, K. Howard, S. Khizroev, and D. Litvinov, J. Appl. Phys. **89**, 7531 (2001).
[90] Y. Hirayama, A. Kikukawa, Y. Honda, N. Shimizu, and M. Futamoto, IEEE Trans. Magn. **36**, 2396 (2000).
[91] Y. Honda, K. Tanahashi, Y. Hirayama, A. Kikukawa, and M. Futamoto, IEEE Trans. Magn. **37**, 1315 (2001).
[92] K. Tanahashi, I. Tamai, S. Matsunuma, T. Kanbe, and A. Ishikawa, J. Appl. Phys. **87**, 6857 (2000).
[93] G. Choe, M. Zheng, E. N. Abarra, B. G. Demczyk, J. N. Zhou, B. R. Acharya, and K. E. Johnson, J. Magn. Magn. Mater. **287**, 159 (2005).
[94] J. W. Park, Y. K. Kim, T. H. Lee, H.-S. Oh, and B.-K. Lee, Phys. Status Solidi A **201**, 1763 (2004).
[95] M. Futamoto, N. Inaba, Y. Hirayama, K. Ito, and Y. Honda, J. Magn. Magn. Mater. **193**, 36 (1999).
[96] T. Shimatsu, H. Uwazumi, Y. Sakai, A. Otsuki, I. Watanabe, H. Muraoka, and Y. Nakamura, IEEE Trans. Magn. **37**, 1567 (2001).
[97] M. Zheng, B. R. Acharya, G. Choe, J. N. Zhou, Z. D. Yang, E. N. Abarra, and K. E. Johnson, IEEE Trans. Magn. **40**, 2498 (2004).
[98] C. H. Lai, and R. F. Jiang, J. Appl. Phys. **93**, 8155 (2003).
[99] S. N. Piramanayagam, J. Z. Shi, H. B. Zhao, C. S. Mah, and J. Zhang, IEEE Trans. Magn. **41**, 3190 (2005).
[100] R. H. Victora, IEEE Trans. Magn. **41**, 537 (2005).
[101] D. Suess, Appl. Phys. Lett. **87**, 012504 (2005)
[102] T. P. Nolan, B. F. Valcu, and H. J. Richter, IEEE Trans. Magn. **47**, 63 (2011).
[103] L. J. Qiu, J. Z. Shi, S. N. Piramanayagam, J. S. Chen, and J. Ding, Thin Solid Films **516**, 5381 (2008).
[104] S. J. Greaves, H. Muraoka, and Y. Kanai, J. Magn. Magn. Mater. **320**, 2889 (2008).
[105] M. H. Kryder, E. C. Gage, T. W. McDaniel, W. A. Challener, R. E. Rottmay, G. Ju, Y. T. Hsia, and M. F. Erden, Proc. IEEE **96**, 1810 (2008).
[106] D. Wachenschwanz, W. Jiang, E. Roddick, A. Homola, P. Dorsey, B. Harper, D. Treves, and C. Bajorek, IEEE Trans. Magn. **41**, 670 (2005).
[107] A. Amer, J. Holliday, D. D. E. Long, E. L. Miller, J.-F. Paris, and T. Schwarz, IEEE Trans. Magn. **47**, 3691 (2011).
[108] H. J. Richter, A. Y. Dobin, K. Gao, O. Heinonen, R. J. Van de Veerdonk, R. T. Lynch, J. Xue, D. K. Weller, P. Asselin, M. F. Erden, and R. M. Brockie, IEEE Trans. Magn. **42**, 2255 (2006).
[109] https://windows101tricks. com/ssd-vs-hdd-which-is-better-for-you/.
[110] http://toshiba.semicon-storage.com/eu/company/news/2015/02/storage-20150224-4.html/.